

# Sensitivity of indirect detection of Neutralino dark matter by Sommerfeld enhancement mechanism

Mikuru Nagayama,<sup>\*</sup> Joe Sato,<sup>†</sup> Yasutaka Takanishi,<sup>‡</sup> and Kazuhiro Tsunemi

*Department of Physics, Saitama University,*

*Shimo-Okubo 255, 338-8570 Saitama Sakura-ku, Japan*

(Dated: January 1, 2022)

## Abstract

We have investigated neutralino dark matter in the framework of minimal supersymmetric Standard Model focusing on the coannihilation region. In this region, where the particle whose mass is tightly degenerated with the neutralino dark matter exists, we can solve the Lithium problem in the case of lepton flavor being violated. It turns out that Sommerfeld enhancement is important in the coannihilation region so that the dark matter signal becomes large enough to be observed by the current sensitivity of indirect experiments.

---

<sup>\*</sup>Electronic address: nagayama@krishna.th.phy.saitama-u.ac.jp

<sup>†</sup>Electronic address: joe@phy.saitama-u.ac.jp

<sup>‡</sup>Electronic address: yasutaka@krishna.th.phy.saitama-u.ac.jp

## I. INTRODUCTION

The discovery of neutrino oscillation in 1998 opens a new era for physics Beyond the Standard Model (SM) [1]. After this discovery, the flavor structure of the lepton sector must be considered and its research becomes a very important topic. On the other hand, another road of Beyond the Standard Model is a quest for Dark Matter (DM) problem. The existence of DM is according to various astrophysical observations, including gravitational effects on the visible matter in the infrared and gravitational lensing of background radiation [2]. Furthermore, the predictions of the SM of cosmology are confirmed by various cosmological observations namely the total mass-energy of Universe contains about 23% DM and 68% of a form of dark energy so that our present Universe contains only about 4% of the “ordinary” matter and energy. However, we do not really know what DM is.

The total abundance of DM, which has important implications for the evolution of the Universe, has been precisely measured by the WMAP collaboration [3] during the last few decades. This requires that a different kind of matter beyond the SM of particle physics must be considered. One of the most popular and most intensive studied candidates is the so-called weakly interacting massive particle (WIMP) that may constitute most of the matter in the Universe [4]. Cosmology provides, therefore, a good motivation for Supersymmetry (SUSY) that has a natural candidate for DM *i.e.* the lightest supersymmetric particle (LSP) can be a stable particle if R-parity conservation is held [5] (for reviews see *e.g.* [6]). As many other physicists have already suggested and studied the scenarios of lightest neutralino being the candidate for LSP in various different frameworks of SUSY models.

We assume that the dark matter particle is neutralino, and we focus on the so-called coannihilation region. In such a region, the mass between LSP neutralino and next-LSP(NLSP) slepton degenerates, we are able to reduce the abundance of DM by an order or more orders of magnitude with a fixed value of DM mass. In addition, Lithium problem [7–9] can be solved if we admit lepton flavor violation [10–15]. For this reason Sommerfeld Enhancement [16–19] effect plays a crucial role in indirect DM observation experiments such as HESS experiment and Fermi-LAT experiment [20, 21]. In fact, this effect has been used in many studies that referred to indirect detection [22–25]. The phenomenon is that the annihilation cross section is enhanced by forming a bound state when DMs move non-relativistically and annihilate into SM particles [26]. Thus our results bring attention to current and future

experiments of astrophysics.

This article is organized as follows: in the next section, we define the Lagrangian related to neutralino and the lightest slepton, and we clarify our notation. In section 3, the method of two-body effective action is reviewed and discussed. Calculations of cross sections and fluxes from dark matter annihilation are also given. In section 4, our calculation results will be presented and discussed. Finally, we conclude in section 5. We summarize the technical details in Appendices A, B, and C.

## II. LAGRANGIAN

In this section, we consider the neutralino-slepton coannihilation region in the framework of Minimal Supersymmetric Standard Model (MSSM). Here we assume that DM is LSP Bino-like neutralino and NLSP are the lightest slepton which is required very tight mass degeneracy with LSP neutralino. It is important to note that we use terminology in this article that the lightest slepton is “stau” because  $\tilde{\ell}_1$  almost consists of right-handed stau in the flavor base.

It is convenient to use a mass base for calculation, so we begin by formulating Lagrangian with this base. In MSSM, neutralino is a linear combination of Higgsino neutral component of  $(\tilde{H}_u^0, \tilde{H}_d^0)$ , Wino neutral component  $(\tilde{W}^0)$ , and Bino  $(\tilde{B}^0)$ . In this base neutralino mass matrix is given by

$$\mathcal{L}_{\text{neutralino mass}} = -\frac{1}{2}(\tilde{\psi}^0)^\top M_N \tilde{\psi}^0 + c.c. \quad (1)$$

Here  $\tilde{\psi}^0 = (\tilde{B}, \tilde{W}^0, \tilde{H}_u^0, \tilde{H}_d^0)^\top$ , and

$$M_N = \begin{pmatrix} M_1 & 0 & -c_\beta s_w m_z & s_\beta s_w m_z \\ 0 & M_2 & c_\beta c_w m_z & -s_\beta c_w m_z \\ -c_\beta s_w m_z & c_\beta c_w m_z & 0 & -\mu \\ s_\beta s_w m_z & -s_\beta c_w m_z & -\mu & 0 \end{pmatrix}, \quad (2)$$

where  $M_1$  is Bino mass,  $M_2$  is Wino mass,  $\mu$  is Higgsino mass,  $m_z$  is  $Z$  boson mass, respectively.  $\theta_w$  is Weinberg angle, and we use shorthand notation:  $s_w = \sin \theta_w$  and  $c_w = \cos \theta_w$ . We also denote  $\tan \beta = v_u/v_d$ , where  $v_u$  and  $v_d$  are vacuum expectation values of  $H_u$  and  $H_d$ , respectively. Also  $s_\beta = \sin \beta$  and  $c_\beta = \cos \beta$ .

The  $\tilde{\psi}^0$  base can be transformed into mass base  $\tilde{\chi}$  using unitary matrix  $(N_{\tilde{G}})_a^b$  ( $a, b = 1, \dots, 4$ ),

$$\tilde{\chi}_a = (N_{\tilde{G}})_a^b \tilde{\psi}^0_b. \quad (3)$$

In this article we do consider only the case of the lightest neutralino being the candidate of DM, thus we fix the value of  $a = 1$ .

The existence of mass degenerated particle with DM in the coannihilation process is necessary, thus we assume such particle being the lightest slepton. This slepton mass matrix follows

$$\mathcal{L}_{\text{slepton mass}} = -\tilde{\psi}_l^\dagger M_{\tilde{l}}^2 \tilde{\psi}_l \quad (4)$$

in flavor base  $\tilde{\psi}_l = (\tilde{e}_L \ \tilde{\mu}_L \ \tilde{\tau}_L \ \tilde{e}_R \ \tilde{\mu}_R \ \tilde{\tau}_R)^\top$ , and  $M_{\tilde{l}}^2$  is given by

$$(M_{\tilde{l}}^2)_{I^J} = \begin{cases} (m_{\tilde{L}}^2)_{I^J} + y_{I^K}^\dagger y_{K^J} v_d^2 + m_z^2 (s_w^2 - 1/2) c_\beta \delta_{I^J} & (\text{for } I, J = 1, 2, 3, K = 4, 5, 6) \\ -\mu v_u y_{I^J}^\dagger + v_d a_{I^J}^\dagger & (\text{for } I = 1, 2, 3, J = 4, 5, 6) \\ -\mu^* v_u y_{I^J} + v_d a_{I^J} & (\text{for } I = 4, 5, 6, J = 1, 2, 3) \\ (m_{\tilde{R}}^2)_{I^J} + y_{I^K} y_{K^J}^\dagger v_d^2 + m_z^2 s_w^2 c_\beta \delta_{I^J} & (\text{for } I, J = 4, 5, 6, K = 1, 2, 3), \end{cases} \quad (5)$$

where  $m_{\tilde{L}}^2, m_{\tilde{R}}^2$  is soft-breaking mass parameter.  $y_I^J$  is Yukawa coupling and  $a_I^J$  is occurred from A-term, where  $I(I = 4, 5, 6)$  represents right-hand subscript and  $J(J = 1, 2, 3)$  represents left-hand superscript, respectively. Note that if we take Hermitian conjugate, right-hand and left-hand are reversed. This base is also changed mass base  $\tilde{l}$  using unitary matrix  $N_{\tilde{l}A}^B$  ( $A, B = 1, \dots, 6$ ),

$$\tilde{l}_A = N_{\tilde{l}A}^B \tilde{\psi}_{lB}, \quad (6)$$

Especially, we assume that the lightest slepton  $\tilde{l}_1$  almost consists of stau  $\tilde{\tau}$ , so we note  $\tilde{l}_1$  as  $\tilde{\tau}$ .

In the same way, we can write down lagrangian of Chargino in the mass base. Chargino is linear combination of Higgsino charged components ( $\tilde{H}_d^-, \tilde{H}_u^+$ ) and Wino charged components ( $\tilde{W}^+, \tilde{W}^-$ ). The mass matrix is written

$$\mathcal{L}_{\text{chargino mass}} = -\frac{1}{2}(\tilde{\psi}^\pm)^\top M_C \tilde{\psi}^\pm + h.c. \quad (7)$$

in  $\tilde{\psi}^\pm = (\tilde{W}^+, \tilde{H}_u^+, \tilde{W}^-, \tilde{H}_d^-)^\top$  base. Here  $M_C$  is

$$M_C = \begin{pmatrix} 0 & X^\top \\ X & 0 \end{pmatrix}, \quad \text{where } X = \begin{pmatrix} M_2 & \sqrt{2}s_\beta m_w \\ \sqrt{2}c_\beta m_w & \mu \end{pmatrix}.$$

By using two unitary matrices  $U$  and  $V$ , the mass base becomes

$$\begin{pmatrix} \tilde{C}_1^+ \\ \tilde{C}_2^+ \end{pmatrix} = V \begin{pmatrix} \tilde{W}^+ \\ \tilde{H}_u^+ \end{pmatrix}, \quad \begin{pmatrix} \tilde{C}_1^- \\ \tilde{C}_2^- \end{pmatrix} = U \begin{pmatrix} \tilde{W}^- \\ \tilde{H}_d^- \end{pmatrix}. \quad (8)$$

The main contributions of Lagrangian which appear in the below diagram are described in the following in terms of the above fields (for reader interest in all interaction, see Appendix A.).

$$\begin{aligned} \mathcal{L} &= \mathcal{L}_{\text{KT}} + \mathcal{L}_{\text{int}} \\ &\sim \frac{1}{2} \tilde{\chi} (i\not{\partial} - m) \tilde{\chi} + \bar{e}^i (i\not{\partial} \delta_i^j - (m_e)_i^j) e_j - \tilde{\tau}^* (\partial^2 + m_\tau^2) \tilde{\tau} \\ &\quad + \frac{1}{2} Z_\mu (\partial^2 + m_Z^2) Z^\mu + \frac{1}{2} A_\mu \partial^2 A^\mu + \mathcal{L}_{\text{gauge}} + \dots, \end{aligned} \quad (9)$$

where  $i, j = 1, 2, 3$  and  $(m_e)_i^j = \text{diag}(m_e, m_\mu, m_\tau)$ . We pick up  $\mathcal{L}_{\text{gauge}}$  as an example of  $\mathcal{L}_{\text{int}}$  which is shown in Eq. (49).  $\mathcal{L}_{\text{gauge}}$  is written in the following form.

$$\begin{aligned} \mathcal{L}_{\text{gauge}} &= ie A_\mu \tilde{\tau}^* \overleftrightarrow{\partial}^\mu \tilde{\tau} - ig_z Z_\mu \left( s_w^2 - \frac{1}{2} N_{\tilde{l}1}^i N_{\tilde{l}i}^{\dagger 1} \right) \tilde{\tau}^* \overleftrightarrow{\partial}^\mu \tilde{\tau} \\ &\quad - i \frac{\sqrt{2}}{2} g \left( W_\mu^+ \tilde{\nu}^{*i} \overleftrightarrow{\partial}^\mu N_{\tilde{l}i}^{\dagger 1} \tilde{\tau} + W_\mu^- \tilde{\tau}^* N_{\tilde{l}1}^i \overleftrightarrow{\partial}^\mu \tilde{\nu}_i \right) \\ &\quad + e^2 A^2 |\tilde{\tau}|^2 + g_z^2 \left( s_w^2 - \frac{1}{2} N_{\tilde{l}1}^i N_{\tilde{l}i}^{\dagger 1} \right)^2 Z^2 |\tilde{\tau}|^2 - 2eg_z \left( s_w^2 - \frac{1}{2} N_{\tilde{l}1}^i N_{\tilde{l}i}^{\dagger 1} \right) A_\mu Z^\mu |\tilde{\tau}|^2 \\ &\quad + \frac{g^2}{2} N_{\tilde{l}1}^i N_{\tilde{l}i}^{\dagger 1} W_\mu^+ W^{-\mu} |\tilde{\tau}|^2, \end{aligned} \quad (10)$$

where the sum of  $i$  is taken from 1 to 3, and we have used the following definition

$$\tilde{\tau}^* \overleftrightarrow{\partial}^\mu \tilde{\tau} = \tilde{\tau}^* \partial^\mu \tilde{\tau} - (\partial^\mu \tilde{\tau}^*) \tilde{\tau}. \quad (11)$$

Here we note  $g$  and  $g'$  as  $SU(2)$  and  $U(1)$  coupling respectively, and  $g = c_w g_z$ .

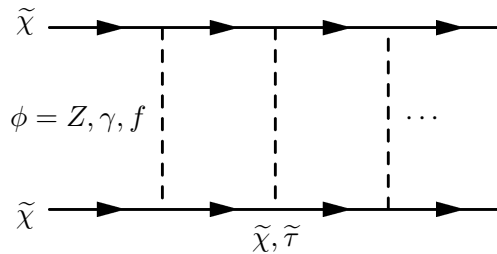


FIG. 1: DM annihilation ladder diagram.  $Z, \gamma$  and  $f$  are taken as an example of  $\phi$ .

### III. FORMALISM

#### A. Two-body effective action

In this section, we derive non-relativistic two-body effective action that has been investigated in Ref. [27]. We will apply their method to calculate the cross sections as of our interest. The steps are as follows: (i) We integrate out the fields except for  $\tilde{\chi}, \tilde{\tau}$ . (ii) We integrate out large momentum mode of  $\tilde{\chi}$  and  $\tilde{\tau}$ . (iii) The non-relativistic action obtained in (ii) is expanded by DM velocity. (iv) We introduce auxiliary fields that represent a two-body state and integrate out all fields except these auxiliary fields.

We begin by integrating out the fields except for  $\tilde{\chi}, \tilde{\tau}$  and obtain 1-loop effective action. For example, we consider integrating out  $A_\mu$ . First, we choose the terms related to  $A_\mu$  from Eq. (9), and get

$$\mathcal{S}_A = -i \ln \int DA \exp i \left[ \int d^4x \left( \frac{1}{2} A_\mu \partial^2 g^{\mu\nu} A_\nu + ie A_\mu \tilde{\tau}^* \overleftrightarrow{\partial}^\mu \tilde{\tau} + e^2 A^2 |\tilde{\tau}|^2 - 2eg_z \left( s_w^2 - \frac{1}{2} N_{\tilde{l}1}^i N_{\tilde{l}i}^{\dagger 1} \right) A_\mu Z^\mu |\tilde{\tau}|^2 \right) \right], \quad (12)$$

where the sum of  $i$  is taken from 1 to 3. Next, we replace  $A_\mu$  by

$$A_\mu \rightarrow A_\mu + i \int d^4y \mathcal{D}_{\mu\nu}^A(x-y) \mathcal{J}^\nu(y)$$

and use the Green function's relation

$$\mathcal{L}_A^{\mu\nu} \mathcal{D}_{\nu\rho}^A(x-y) = i\delta(x-y)\delta_\rho^\mu. \quad (13)$$

Then Eq. (12) becomes

$$\mathcal{S}_A = -i \ln \text{Det}^{-\frac{1}{2}}(-\mathcal{L}_A^{\mu\nu}) + \frac{i}{2} \int d^4x d^4y \mathcal{J}^\mu(x) \mathcal{D}_{\mu\nu}^A(x-y) \mathcal{J}^\nu(y), \quad (14)$$

where

$$\begin{aligned} \mathcal{L}_A^{\mu\nu} &= (\partial^2 + 2e^2 |\tilde{\tau}|^2) g^{\mu\nu}, \\ \mathcal{J}^\mu(x) &= ie \tilde{\tau}^* \overleftrightarrow{\partial}^\mu \tilde{\tau} - 2eg_z \left( s_w^2 - \frac{1}{2} N_{\tilde{l}1}^i N_{\tilde{l}i}^{\dagger 1} \right) Z^\mu |\tilde{\tau}|^2. \end{aligned}$$

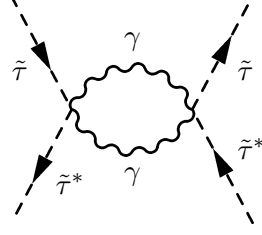


FIG. 2: 1-loop interaction diagram mediated by photons.

Here, we replace the first term of Eq. (14) as follows.

$$\begin{aligned}
-i \ln \text{Det}^{-\frac{1}{2}}(-\mathcal{L}_A^{\mu\nu}) &= \frac{i}{2} \text{Tr} [\ln (-\partial^2 - 2e^2 |\tilde{\tau}|^2) g^{\mu\nu}] \\
&\equiv \frac{i}{2} \text{Tr} [\ln (A_0 + \delta A)] \\
&= \frac{i}{2} \text{Tr} \left[ \ln A_0 + A_0^{-1} \delta A - \frac{1}{2} A_0^{-1} \delta A A_0^{-1} \delta A \right] \\
&\sim i e^4 \text{tr} \int d^4 x_1 d^4 x_2 |\tilde{\tau}|^2(x_1) |\tilde{\tau}|^2(x_2) D_{\mu\nu}^A(x_1 - x_2) D^{A\nu\rho}(x_2 - x_1). \quad (15)
\end{aligned}$$

Note that  $\text{Tr}()$  donates operator trace and  $\text{tr}()$  donates Dirac trace. Also  $D_{\mu\nu}^A(x - y)$  represents photon propagator,

$$A_0^{-1} = i D_{\mu\nu}^A(x - y) = i \int \frac{d^4 q}{(2\pi)^4} \frac{-i g_{\mu\nu}}{q^2 + i\epsilon} e^{-iq(x-y)}. \quad (16)$$

The second term of Eq. (14),  $\mathcal{D}_{\mu\nu}^A \sim D_{\mu\nu}^A$  at the lowest order of expansion. Finally, we get effective action on  $A_\mu$  as follows

$$\begin{aligned}
\mathcal{S}_A &= i e^4 \text{tr} \int d^4 x_1 d^4 x_2 |\tilde{\tau}|^2(x_1) |\tilde{\tau}|^2(x_2) D_{\mu\nu}^A(x_1 - x_2) D^{A\nu\rho}(x_2 - x_1) \\
&\quad + \frac{i}{2} \int d^4 x d^4 y \mathcal{J}^\mu(x) D_{\mu\nu}^A(x - y) \mathcal{J}^\nu(y). \quad (17)
\end{aligned}$$

By this calculation, we can represent the 1-loop interaction shown in Fig. 2.

After all fields except  $\tilde{\chi}, \tilde{\tau}$  are integrated out, the effective action becomes

$$\begin{aligned}
\mathcal{S}_{eff} &= \int d^4 x \left[ \frac{1}{2} \tilde{\chi} (i\not{\partial} - m) \tilde{\chi} - \tilde{\tau}^* (\partial^2 + m_\tau^2) \tilde{\tau} \right] \\
&\quad + \mathcal{S}'_A + \mathcal{S}_Z + \mathcal{S}'_W + \mathcal{S}'_{\tilde{\nu}} + \mathcal{S}_e + \mathcal{S}_{\tilde{C}} + \mathcal{S}_{h^0}. \quad (18)
\end{aligned}$$

One can see other action of  $\mathcal{S}_A$  in Appendix B.

Next, we integrate out the large momentum modes of  $\tilde{\chi}, \tilde{\tau}$ . Here we divide the fields two

parts, namely relativistic part and non-relativistic part. For the case of  $\tilde{\chi}$ , it will be

$$\begin{aligned}\tilde{\chi}(x) &= \tilde{\chi}(x)_R + \tilde{\chi}(x)_{NR}, \\ \tilde{\chi}(x)_R &= \int_R \frac{d^4q}{(2\pi)^4} \phi^0(q) e^{-iqx}, \\ \tilde{\chi}(x)_{NR} &= \int_{NR} \frac{d^4q}{(2\pi)^4} \phi^0(q) e^{-iqx},\end{aligned}\tag{19}$$

where  $\phi^0$  is the Fourier coefficient of the DM field. After this division, we integrate out  $\tilde{\chi}_R$ . The same operation is done for  $\tilde{\tau}$ , in the result we obtain

$$\mathcal{S}_{NR} = \int d^4x \left[ \frac{1}{2} \tilde{\chi}_{NR} (i\not{\partial} - m) \tilde{\chi}_{NR} - \tilde{\tau}_{NR}^* (\partial^2 + m_{\tilde{\tau}}^2) \tilde{\tau}_{NR} \right] + \mathcal{S}_{Pot}(\tilde{\chi}_{NR}, \tilde{\tau}_{NR}) + \mathcal{S}_{Im}(\tilde{\chi}_{NR}, \tilde{\tau}_{NR}),\tag{20}$$

Here we note  $\mathcal{S}_{Pot}$  is the real part except the kinematic part, and  $\mathcal{S}_{Im}$  is the imaginary part. In the following, we omit the subscript NR for  $\tilde{\chi}$  and  $\tilde{\tau}$ .

Then, we expand this action by DM velocity. For this expansion, we use two-component spinors of neutralino and stau. These spinor fields are defined in the following form.

$$\bar{\chi} = \begin{pmatrix} e^{-imt} \zeta + i e^{imt} \frac{\vec{\nabla} \cdot \sigma}{2m} \zeta^c \\ e^{imt} \zeta^c - i e^{-imt} \frac{\vec{\nabla} \cdot \sigma}{2m} \zeta \end{pmatrix}, \quad \tilde{\tau} = \frac{1}{\sqrt{2m}} \eta e^{-imt} + \frac{1}{\sqrt{2m}} \xi e^{imt},\tag{21}$$

where  $\zeta^c = -i\sigma^2 \zeta^{\dagger T}$ . In this form,  $\mathcal{S}_{NR}$  becomes

$$\mathcal{S}_{NR} = \mathcal{S}_{KT} + \mathcal{S}_{Pot} + \mathcal{S}_{Im},\tag{22}$$

where

$$\begin{aligned}\mathcal{S}_{KT} &= \frac{1}{2} \int d^4x \bar{\chi}(x) (i\not{\partial} - m) \chi(x) - \int d^4x \tilde{\tau}^* (\partial^2 + m_{\tilde{\tau}}^2) \tilde{\tau} \\ &= \int d^4x \left[ \zeta^\dagger \left( i\partial_0 + \frac{\nabla^2}{2m} \right) \zeta + \eta^* \left( i\partial_0 + \frac{\nabla^2}{2m} - \delta m \right) \eta - \xi^* \left( i\partial_0 - \frac{\nabla^2}{2m} + \delta m \right) \xi \right].\end{aligned}\tag{23}$$

We define to quantify  $\delta m$  as

$$\delta m = \frac{m_{\tilde{\tau}}^2 - m^2}{2m},\tag{24}$$



and the potential part,

$$\begin{aligned}
\mathcal{S}_{Pot} &= \int d^4x d^4y \delta(x^0 - y^0) \left[ \frac{\alpha}{r} + g_z^2 \left( s_w^2 - \frac{1}{2} N_{\tilde{l}^1}^i N_{\tilde{l}^i}^{\dagger 1} \right)^2 \frac{e^{-m_z r}}{4\pi r} + C_{h^0}^2 \frac{e^{-(m_{h^0})r}}{8\pi m^2} \right] \eta^*(x) \eta(x) \xi^*(y) \xi(y) \\
&+ \int d^4x d^4y \frac{e^{-m_e r} \delta(x^0 - y^0)}{16\pi m r} \left( C_1^i(m_e)_i^j C_{2j}^\dagger - C_2^i(m_e)_i^j C_{1j}^\dagger \right) \\
&\times (\eta^*(x) \zeta^{c\dagger}(x) \xi(y) \zeta(y) - \xi^*(x) \zeta^\dagger(x) \eta(y) \zeta^c(y)) \\
&\equiv \int d^4x d^4y \delta(x^0 - y^0) \left[ \mathcal{S}_{Pot}^{(1)} \eta^*(x) \eta(x) \xi^*(y) \xi(y) \right. \\
&\left. + \mathcal{S}_{Pot}^{(2)} (\eta^*(x) \zeta^{c\dagger}(x) \xi(y) \zeta(y) - \xi^*(x) \zeta^\dagger(x) \eta(y) \zeta^c(y)) \right], \tag{25}
\end{aligned}$$

where  $i, j = 1, 2, 3$  and the sum of  $i$  is taken from 1 to 3. Note that  $C_1^i, C_2^i$  and  $C_{h^0}$  are defined as in Eq. (66), Eq. (67), and Eq. (75), respectively, in Appendix B. Also, the imaginary part becomes

$$\mathcal{S}_{Im} = \mathcal{S}_\gamma + \mathcal{S}_e + \mathcal{S}_Z + \mathcal{S}_{Zh^0} + \mathcal{S}_{h^0} + \mathcal{S}_W + \mathcal{S}_\nu. \tag{26}$$

For example,  $\mathcal{S}_\gamma$  is calculated the diagram drawn above (see Fig. 2) by optical theorem, then we obtain

$$\begin{aligned}
\mathcal{S}_\gamma &= i \frac{e^4}{8\pi m^2} \int d^4x \eta^*(x) \eta(x) \xi^*(x) \xi(x) \\
&\equiv i \Gamma_{\gamma\gamma} \int d^4x \eta^*(x) \eta(x) \xi^*(x) \xi(x). \tag{27}
\end{aligned}$$

One can see the other actions except for  $\mathcal{S}_\gamma$  in Appendix C.

Next, we introduce auxiliary fields  $\sigma_{\tilde{\chi}}, \sigma_{\tilde{\tau}}$  to make two-body states  $\tilde{\chi}\tilde{\chi}$  and  $\tilde{\tau}\tilde{\tau}$ , which satisfy the relationship:

$$\begin{aligned}
1 &= \int D\sigma_{\tilde{\tau}} Ds_{\tilde{\tau}}^\dagger \exp \left[ \frac{i}{2} \int d(xy) \sigma_{\tilde{\tau}}(t, \mathbf{x}, \mathbf{y}) \left( s_{\tilde{\tau}}^\dagger(t, \mathbf{x}, \mathbf{y}) - i\eta^*(t, \mathbf{x}) \xi(t, \mathbf{y}) \right) \right], \\
1 &= \int D\sigma_{\tilde{\tau}}^\dagger Ds_{\tilde{\tau}} \exp \left[ \frac{i}{2} \int d(xy) \sigma_{\tilde{\tau}}^\dagger(t, \mathbf{x}, \mathbf{y}) \left( s_{\tilde{\tau}}(t, \mathbf{x}, \mathbf{y}) - i\xi^*(t, \mathbf{y}) \eta(t, \mathbf{x}) \right) \right], \\
1 &= \int D\sigma_{\tilde{\chi}} Ds_{\tilde{\chi}}^\dagger \exp \left[ \frac{i}{2} \int d(xy) \sigma_{\tilde{\chi}}(t, \mathbf{x}, \mathbf{y}) \left( s_{\tilde{\chi}}^\dagger(t, \mathbf{x}, \mathbf{y}) - \frac{1}{2} \zeta^\dagger(t, \mathbf{x}) \zeta^c(t, \mathbf{y}) \right) \right], \\
1 &= \int D\sigma_{\tilde{\chi}}^\dagger Ds_{\tilde{\chi}} \exp \left[ \frac{i}{2} \int d(xy) \sigma_{\tilde{\chi}}^\dagger(t, \mathbf{x}, \mathbf{y}) \left( s_{\tilde{\chi}}(t, \mathbf{x}, \mathbf{y}) - \frac{1}{2} \zeta^{c\dagger}(t, \mathbf{y}) \zeta(t, \mathbf{x}) \right) \right],
\end{aligned}$$

where  $d(xy) = dt d^3x d^3y$ . With this relationship, we integrate out the fields except for  $\sigma_{\tilde{\chi}}$

and  $\sigma_{\tilde{\tau}}$ . Then two-body state effective action is obtained as

$$\mathcal{S}^H = \int d^4x d^3r \Phi^\dagger(x, \mathbf{r}) \left( \frac{\nabla_{\tilde{\tau}}^2}{m} + i\partial_{x^0} + \frac{\nabla_x^2}{4m} - \begin{pmatrix} 2\delta m & 0 \\ 0 & 0 \end{pmatrix} + \frac{1}{2} \begin{pmatrix} -1 & 0 \\ 0 & 1 \end{pmatrix} \mathcal{V} \right) \Phi(x, \mathbf{r}), \quad (28)$$

where  $\Phi(x, \mathbf{r})$  is represented as

$$\Phi(x, \mathbf{r}) = \mathcal{V}^{-1} \begin{pmatrix} \sigma_{\tilde{\tau}}(x, \mathbf{r}) \\ \sigma_{\tilde{\chi}}(x, \mathbf{r}) \end{pmatrix}, \quad \mathcal{V} = \begin{pmatrix} -2\mathcal{S}_{Pot}^{(1)} - 2i\delta(\mathbf{x} - \mathbf{y})\Gamma & -4i\mathcal{S}_{Pot}^{(2)} \\ 4i\mathcal{S}_{Pot}^{(2)} & 0 \end{pmatrix}. \quad (29)$$

Note that  $x$  denotes the center of mass coordinate in two-body system and  $\mathbf{r}$  is the relative coordinate, and here we note  $\Gamma$  as

$$\Gamma = \Gamma_{e_i e_i} + \Gamma_{\gamma\gamma} + \Gamma_{Z^0 Z^0} + \Gamma_{Z^0 \gamma} + \Gamma_{Z^0 h^0} + \Gamma_{h^0 h^0} + \Gamma_{\nu_i \nu_i}. \quad (30)$$

The symbols  $\Gamma_f$  ( $f = e_i e_i, \gamma\gamma, Z^0 Z^0, Z^0 \gamma, Z^0 h^0, h^0 h^0, \nu_i \nu_i$ ) are listed in Appendix C.

## B. cross section

In this subsection, we calculate DM annihilation cross section with the method written in [27, 28]. For S-wave, annihilation cross section is obtained by determining radial component of Green function which satisfies Schwinger-Dyson equation derived from Eq. (28):

$$\left[ \frac{\nabla_{\tilde{\tau}}^2}{m} + i\partial_{x^0} + \frac{\nabla_x^2}{4m} - \mathbf{V}(\mathbf{r}) + i\Gamma \frac{\delta(r)}{4\pi r} \right] \langle 0 | T \Phi(x, \mathbf{r}) \Phi^\dagger(y, \mathbf{r}') | 0 \rangle = i\delta(x - y) \delta(\mathbf{r} - \mathbf{r}'), \quad (31)$$

where  $\mathbf{V}(\mathbf{r})$  is

$$\mathbf{V}(\mathbf{r}) = \begin{pmatrix} 2\delta m - \mathcal{S}_{Pot}^{(1)} & -2i\mathcal{S}_{Pot}^{(2)} \\ -2i\mathcal{S}_{Pot}^{(2)} & 0 \end{pmatrix}. \quad (32)$$

By defining the radial component of Green function as  $\mathbf{G}^{(E,l)}$ , Eq. (31) becomes the following form.

$$\left[ -E - \frac{1}{mr} \frac{d^2}{dr^2} r + \mathbf{V}(\mathbf{r}) - i\Gamma \frac{\delta(r)}{4\pi r} \right] \mathbf{G}^{(E,0)}(r, r') = \frac{\delta(r - r')}{r^2}. \quad (33)$$

To determine  $\mathbf{G}^{(E,0)}$ , Eq. (33) must be solved in a proper boundary condition. For this purpose we consider the terms involved  $\Gamma$  as in perturbation series and by using variable

transformation  $\mathbf{g}(r, r') = rr' \mathbf{G}_{ii}^{(E,0)}(r, r')$ . The leading order's solution  $\mathbf{g}_0(r, r')$  satisfies the equation

$$-\frac{1}{m} \frac{d^2}{dr^2} \mathbf{g}_0(r, r') + \mathbf{V}(\mathbf{r}) \mathbf{g}_0(r, r') - E \mathbf{g}_0(r, r') = \delta(r - r'). \quad (34)$$

We get  $\mathbf{g}_0(r, r')$  in the following form:

$$\mathbf{g}_0(r, r') = m \mathbf{g}_>(r) \mathbf{g}_<^\top(r') \theta(r - r') + m \mathbf{g}_<(r) \mathbf{g}_>^\top(r') \theta(r' - r). \quad (35)$$

Here The solutions  $\mathbf{g}_>(r)$  and  $\mathbf{g}_<(r)$  satisfy the below boundary condition written in [27].

(i)  $\mathbf{g}_<(0) = \mathbf{0}$  ,  $\frac{d \mathbf{g}_<(0)}{dr} = \mathbf{1}$  ,

(ii)  $\mathbf{g}_>(0) = \mathbf{1}$  ,  $\mathbf{g}_>(r)$  has only outgoing wave at  $r \rightarrow \infty$ .

Also,  $\mathbf{g}_{<(>)}(r)$  satisfies, respectively, the following differential equation

$$-\frac{1}{m} \frac{d^2}{dr^2} \mathbf{g}_{<(>)}(r) + \mathbf{V}(\mathbf{r}) \mathbf{g}_{<(>)}(r) = E \mathbf{g}_{<(>)}(r). \quad (36)$$

Furthermore,  $\tilde{\tau}$  does not exist at  $r \rightarrow \infty$  when  $E < 2\delta m$ , so

$$[\mathbf{g}_>(r)]_{ij} \Big|_{r \rightarrow \infty} = \delta_{i2} d_{2j}(E) e^{i\sqrt{mE}r}. \quad (37)$$

When we calculate  $\mathbf{g}_>(r)$  by using the first-order perturbation, cross section for annihilation channel  $f$  can be written as

$$\sigma_2^{(S)} v|_f = [\tilde{\Gamma}_f]_{11} d_{21}(mv^2/4) d_{21}^*(mv^2/4). \quad (38)$$

In addition, when we write the sum of each annihilation channel  $f$  as  $\Gamma = \sum_f \tilde{\Gamma}_f$ , total cross section satisfies

$$\sigma_2^{(S)} v = \Gamma_{11} d_{21}(mv^2/4) d_{21}^*(mv^2/4). \quad (39)$$

Therefore it is necessary to solve the equation about  $\mathbf{g}_>(r)$  to determine  $d_{2j}$  and cross section.

### C. DM signature

Next, we calculate gamma-ray flux from DM annihilation that occurred in our galactic center. The spectrum of gamma-ray has two types. One of these is the line gamma-ray

spectrum and the other is the continuum gamma-ray spectrum. Because the DM moves non-relativistically, the line spectrum lies at the mass of DM. On the other hand, continuum gamma-ray signal comes from jets from the DM annihilation. For example, produced  $\pi$  mesons from DM annihilation decay into  $\gamma\gamma$ . Such a signal is useful when the cosmic background is well known.

The gamma-ray flux from DM annihilation used by indirect detection experiments [29, 30] is given by

$$\frac{d\Phi_\gamma}{dE} = \frac{1}{4\pi} \frac{1}{m_\chi^2} \sum_f \frac{dN_f}{dE} \frac{\langle\sigma v\rangle_f}{2} \times J, \quad (40)$$

where  $m_\chi$  is DM mass, and  $dN_f/dE \cdot dE$  is the numbers of photon derived from annihilation channel  $f$  whose energy is between  $E$  and  $E + dE$ .  $\langle\sigma v\rangle$  is the DM annihilation cross section averaged with the velocity.

$J$  is called “ $J$ -factor” which is determined by an astrophysical parameter and is given as

$$J = \int_{\text{line of sight}} dl(\theta) \int_{\Delta\Omega} d\Omega \rho^2, \quad (41)$$

where  $\Delta\Omega$  is the angular resolution and  $\rho$  is DM density in our galaxy. N-body simulations show some DM halo profiles. For example, NFW [31], Burkert [32], and Einasto [33, 34] profiles are widely used.

$$\rho_{\text{NFW}} = \frac{\rho_s}{(r/r_s)(1 + r/r_s)^2}, \quad (42)$$

$$\rho_{\text{Burkert}} = \frac{\rho_s}{(1 + r/r_s)(1 + (r/r_s)^2)}, \quad (43)$$

$$\rho_{\text{Einasto}} = \rho_s \exp \left\{ -\frac{2}{\alpha} \left[ \left( \frac{r}{r_s} \right)^\alpha - 1 \right] \right\}. \quad (44)$$

Here  $\rho_s$ ,  $r_s$ , and  $\alpha$  are determined from observations [35]. Next, we discuss quantities determined from particle physics. Cross section  $\langle\sigma v\rangle$  is determined from Eq. (38) as mentioned above. We calculate energy spectrum  $dN_f/dE$  with pythia [36] for each annihilation channels.

For the case  $Z$ -boson annihilate to gamma is shown in Fig. 3.

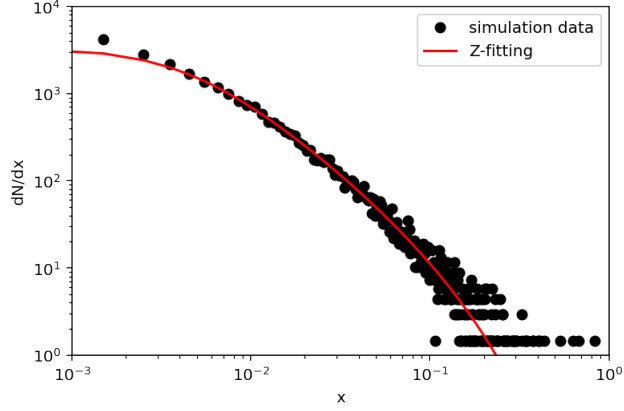


FIG. 3: Energy spectrum in the case where DM decays into  $Z$ -boson.

$$\frac{dN_Z}{dx} = \frac{0.642e^{-7.98x}}{x^{1.59} + 1.88 \times 10^{-4}}, \quad (45)$$

where  $x = E/m_\chi$ .

For the case  $W$ -boson and  $\tau$  annihilate to gamma is respectively shown in Fig. 4.

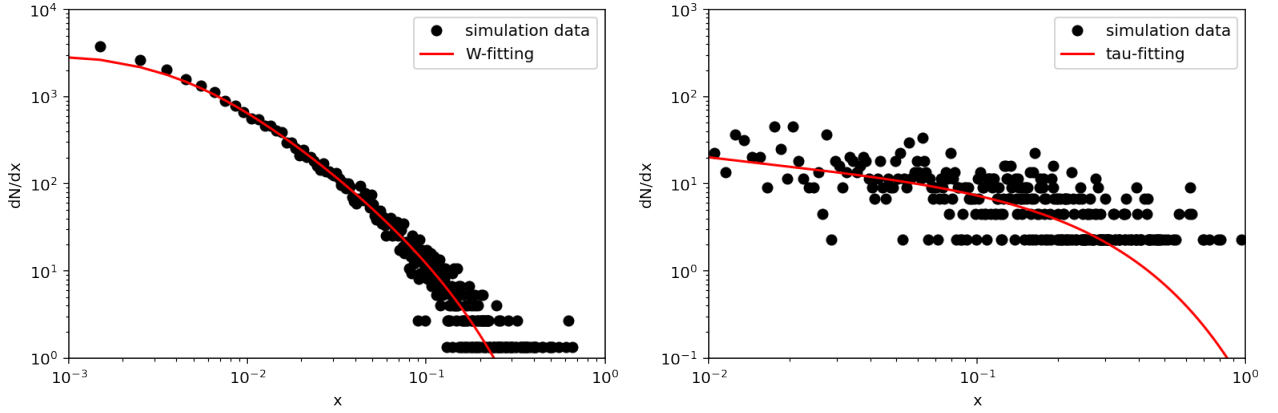


FIG. 4: The left graph corresponds to the case where DM decays into  $W$ -boson. The right graph corresponds to the case where DM decays into  $\tau$ .

$$\frac{dN_W}{dx} = \frac{0.931e^{-8.60x}}{x^{1.49} + 2.87 \times 10^{-4}}, \quad \frac{dN_\tau}{dx} = \frac{0.0264e^{-5.24x}}{x^{3.89 \times 10^{-4}} - 0.997}. \quad (46)$$

For directly decaying into  $\gamma\gamma$  case, the spectrum becomes

$$\frac{dN_\gamma}{dE} = 2\delta(E - m). \quad (47)$$

## IV. RESULT

In this section, we will discuss our results. First, we find that the peak of cross section appears with the fixed value of  $\delta m$  by using the parameters which are presented in the following tables for numerical calculations [37]: The dimensionless parameters are shown in Table 1 and the dimensionful parameters are shown in GeV units in Table 2 and the mixing parameters are shown in Table 3, Table 4 and Table 5. These parameters are satisfied with a positive solution for Li problem in cosmology. We should keep in our mind the fact that stau mass is limited up to about 430 GeV by ATLAS experiment [38]. Thus we have to set up the mass parameters of neutralino and stau to adjust peak position at near 430 GeV. We assume, however, that the calculation results are not affected if the mass values are slightly different from the values in the tables.

parameter	$g$	$g'$	$s_w^2$	$\tan \beta$	$\cot \alpha$	$y_1^1$	$y_2^2$	$y_3^3$
value	0.6387	0.3623	0.23	24.21	-24.21	$1.0 \times 10^{-5}$	$1.5 \times 10^{-2}$	0.2542

TABLE I: Dimensionless parameters for numerical calculations [37] are presented.

parameter	$m$	$m_{\tilde{\tau}}$	$m_{C_1}$	$\mu$	$A_0$	$m_{e \times 10^{-3}}$	$m_\mu$	$m_\tau$	$v$	$m_w$	$m_z$	$m_{h^0}$
value	379.596576	379.606567	725.76	1.776	-3098.1	0.511	0.105	1.776	243.5786	80.2	91.19	125.18

TABLE II: The mass parameters used for numerical calculations are presented in GeV unit [37].

chargino					
real part			imaginary part		
$\text{Re}U_i^j$	$j=1$	$j=2$	$\text{Im}U_i^j$	$j=1$	$j=2$
$i=1$	$-9.97043970 \times 10^{-1}$	$7.68330827 \times 10^{-2}$	$i=1$	$-2.92376714 \times 10^{-16}$	$9.05483611 \times 10^{-18}$
$i=2$	$7.68330827 \times 10^{-2}$	$9.97043970 \times 10^{-1}$	$i=2$	$-4.61092153 \times 10^{-17}$	$-7.73222256 \times 10^{-16}$
$\text{Re}V_i^j$	$j=1$	$j=2$	$\text{Im}V_i^j$	$j=1$	$j=2$
$i=1$	$-9.99396601 \times 10^{-1}$	$3.47337437 \times 10^{-2}$	$i=1$	$7.74343187 \times 10^{-16}$	$0.00000000 \times 10^0$
$i=2$	$3.47337437 \times 10^{-2}$	$9.99396601 \times 10^{-1}$	$i=2$	$0.00000000 \times 10^0$	$7.74343187 \times 10^{-16}$

TABLE III: The values of the unitary matrix that diagonalizes chargino.

neutralino				
real part				
$\text{Re}N_{\tilde{G}^a}^b$	$b = 1$	$b = 2$	$b = 3$	$b = 4$
$a = 1$	$9.99599220 \times 10^{-1}$	$-2.13656993 \times 10^{-3}$	$2.72724410 \times 10^{-2}$	$-7.28340424 \times 10^{-3}$
$a = 2$	$3.78724402 \times 10^{-3}$	$9.98231872 \times 10^{-1}$	$-5.41258402 \times 10^{-2}$	$2.42730150 \times 10^{-2}$
$a = 3$	$-2.23811821 \times 10^{-17}$	$4.82387775 \times 10^{-17}$	$6.11227032 \times 10^{-16}$	$-6.11568206 \times 10^{-16}$
$a = 4$	$2.42682988 \times 10^{-2}$	$-5.55057268 \times 10^{-2}$	$-7.05176402 \times 10^{-1}$	$7.06439245 \times 10^{-1}$
imaginary part				
$\text{Im}N_{\tilde{G}^a}^b$	$b = 1$	$b = 2$	$b = 3$	$b = 4$
$a = 1$	$-5.13227991 \times 10^{-16}$	$2.88642911 \times 10^{-19}$	$-1.03992019 \times 10^{-17}$	$-1.74565311 \times 10^{-18}$
$a = 2$	$-1.78170707 \times 10^{-18}$	$-2.33972913 \times 10^{-16}$	$5.73625399 \times 10^{-18}$	$1.43366353 \times 10^{-18}$
$a = 3$	$1.40749921 \times 10^{-2}$	$-2.11584124 \times 10^{-2}$	$-7.06436727 \times 10^{-1}$	$-7.07319847 \times 10^{-1}$
$a = 4$	$5.84094614 \times 10^{-18}$	$-8.37388039 \times 10^{-18}$	$-6.12074422 \times 10^{-16}$	$-6.13058014 \times 10^{-16}$

TABLE IV: The values of the diagonalizing unitary matrix of neutralino.

slepton						
real part						
$\text{Re}N_{\tilde{L}^A}^B$	$B = 1$	$B = 2$	$B = 3$	$B = 4$	$B = 5$	$B = 6$
$A = 1$	$-6.31168044 \times 10^{-9}$	$2.63719358 \times 10^{-6}$	$-1.71009221 \times 10^{-1}$	$6.25408690 \times 10^{-11}$	$-5.57777646 \times 10^{-8}$	$-9.85269428 \times 10^{-1}$
$A = 2$	$-4.88052654 \times 10^{-6}$	$-1.47061845 \times 10^{-2}$	$1.26260288 \times 10^{-5}$	$-2.05256544 \times 10^{-8}$	$-7.02536796 \times 10^{-1}$	$-2.18090514 \times 10^{-6}$
$A = 3$	$-1.68078331 \times 10^{-5}$	$-2.88036700 \times 10^{-8}$	$-1.53915085 \times 10^{-10}$	$-1.65361745 \times 10^{-1}$	$2.67385497 \times 10^{-8}$	$-4.95673580 \times 10^{-11}$
$A = 4$	$1.00627884 \times 10^{-7}$	$-5.03237436 \times 10^{-5}$	$9.85269426 \times 10^{-1}$	$-3.17467808 \times 10^{-10}$	$1.00201302 \times 10^{-5}$	$-1.71009221 \times 10^{-1}$
$A = 5$	$6.62240877 \times 10^{-2}$	$6.99028792 \times 10^{-1}$	$7.13839275 \times 10^{-5}$	$-6.76095272 \times 10^{-6}$	$-1.46315410 \times 10^{-2}$	$-8.58412190 \times 10^{-6}$
$A = 6$	$-8.24980621 \times 10^{-1}$	$5.55284568 \times 10^{-2}$	$5.85237100 \times 10^{-6}$	$8.39260849 \times 10^{-5}$	$-1.15816598 \times 10^{-3}$	$-7.02385695 \times 10^{-7}$
imaginary part						
$\text{Im}N_{\tilde{L}^A}^B$	$B = 1$	$B = 2$	$B = 3$	$B = 4$	$B = 5$	$B = 6$
$A = 1$	$-6.69074517 \times 10^{-9}$	$2.68186615 \times 10^{-6}$	$-3.36466824 \times 10^{-15}$	$-6.50682427 \times 10^{-11}$	$-7.01708566 \times 10^{-8}$	$4.44552436 \times 10^{-23}$
$A = 2$	$3.55520850 \times 10^{-6}$	$-1.48888937 \times 10^{-2}$	$-5.52344800 \times 10^{-8}$	$1.51693448 \times 10^{-8}$	$-7.11339651 \times 10^{-1}$	$6.71707263 \times 10^{-16}$
$A = 3$	$1.00325957 \times 10^{-4}$	$-4.18395754 \times 10^{-10}$	$2.93857601 \times 10^{-10}$	$9.86232976 \times 10^{-1}$	$6.16275932 \times 10^{-10}$	$1.39096557 \times 10^{-17}$
$A = 4$	$1.44670207 \times 10^{-7}$	$-5.11527461 \times 10^{-5}$	$1.15540529 \times 10^{-12}$	$7.71687277 \times 10^{-11}$	$1.02274109 \times 10^{-5}$	$-9.52745431 \times 10^{-21}$
$A = 5$	$-4.78727158 \times 10^{-2}$	$7.10102998 \times 10^{-1}$	$-8.62478816 \times 10^{-9}$	$4.88605503 \times 10^{-6}$	$-1.48648974 \times 10^{-2}$	$1.39571889 \times 10^{-17}$
$A = 6$	$5.59222261 \times 10^{-1}$	$5.99258994 \times 10^{-2}$	$3.23933295 \times 10^{-10}$	$-5.68738081 \times 10^{-5}$	$-1.24999822 \times 10^{-3}$	$1.05557136 \times 10^{-18}$

TABLE V: The values of the real part and imaginary part of diagonalizing unitary matrix of slepton.

We calculate for several annihilation channels. (1) we show the result of the cross sections DM decaying directly into two gammas for the corresponding  $\delta m$  as displayed in Fig. 5.

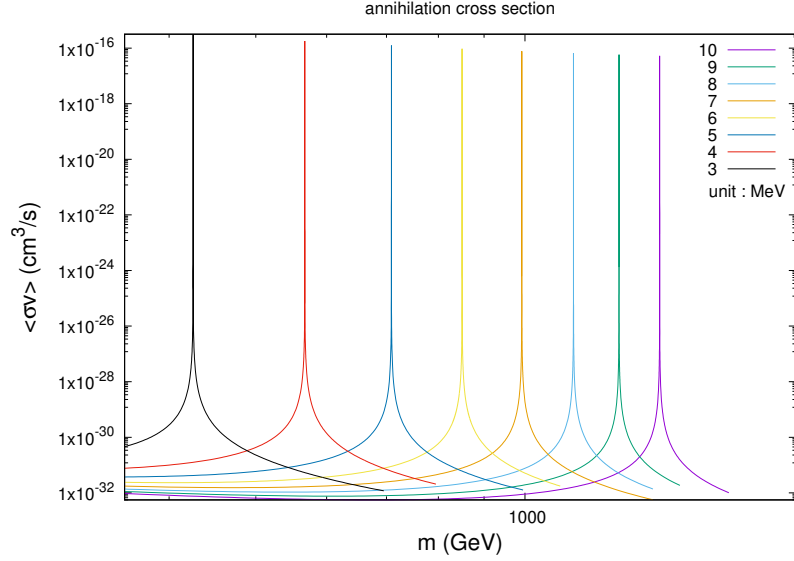


FIG. 5: Annihilation cross section to photons per  $\delta m$ . Each graph name represents  $\delta m$  in MeV units.

From Fig. 5 we realize that annihilation cross sections reach the height point at different DM mass, and the cross sections decrease as its  $\delta m$  increases. (2) cross section of DM decaying directly into  $Z$ -boson,  $W$ -boson, and  $\tau$  are shown in Fig. 6 and Fig. 7, respectively.

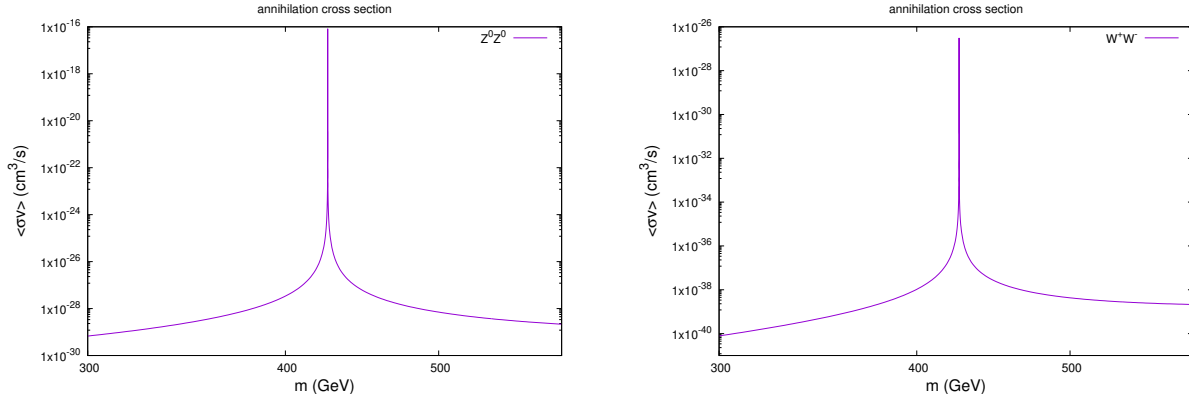


FIG. 6: The left(right) plot correspond to annihilating  $Z^0 Z^0(W^+ W^-)$  case, where we set  $\delta m = 3$  MeV.



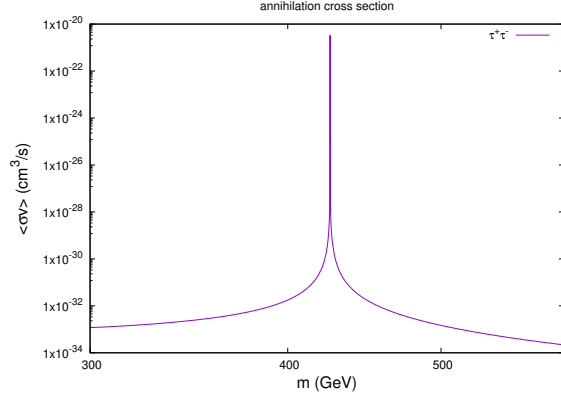


FIG. 7: Annihilation cross section to  $\tau$ . Here we set  $\delta m = 3$  MeV.

As an example of continuum flux, the case where the DM decays into  $Z^0 Z^0$ ,  $W^+ W^-$  is shown in Fig. 8. Here  $J$ -factor and angular resolution are referred from [39].

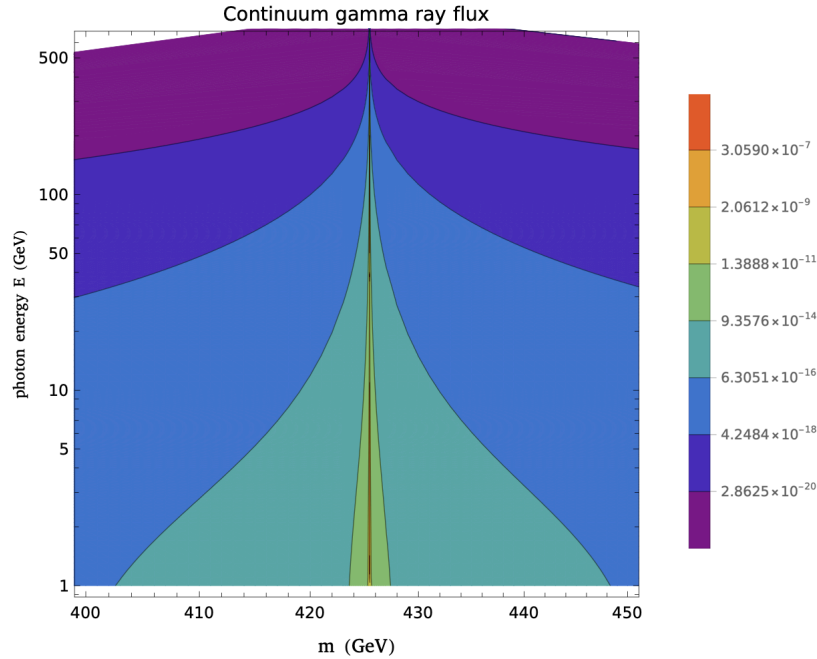


FIG. 8: Continuum gamma-ray flux in the unit of  $(\text{cm}^{-2}\text{sec}^{-1}\text{GeV}^{-1})$  when DM decays into  $Z^0 Z^0$ ,  $W^+ W^-$ . The color of the graph describes the size of flux. Here, it is set to  $\delta m = 3$  MeV,  $J = 1 \times 10^{20} \text{ GeV}^2/\text{cm}^5$ ,  $\Delta\Omega = 1 \times 10^{-5}$ .

In Fig. 8, the horizontal axis represents DM mass and the vertical axis represents observed photon energy. The color of the figure means the size of flux which is larger at the peak

position of the cross section and low photon energy and becomes smaller as the distance increases.

We compare our result to HESS experimental data of  $\chi\chi \rightarrow \gamma\gamma$  focusing on coannihilation region. The graph represented this is shown in Fig. 9. As we can see from this figure cross section invades the prohibited area, therefore we can constrain the parameter in our model. We also show the sensitivity projected by CTA [40]. Using this restricted parameter, we are able to constrain the parameters even more than now.

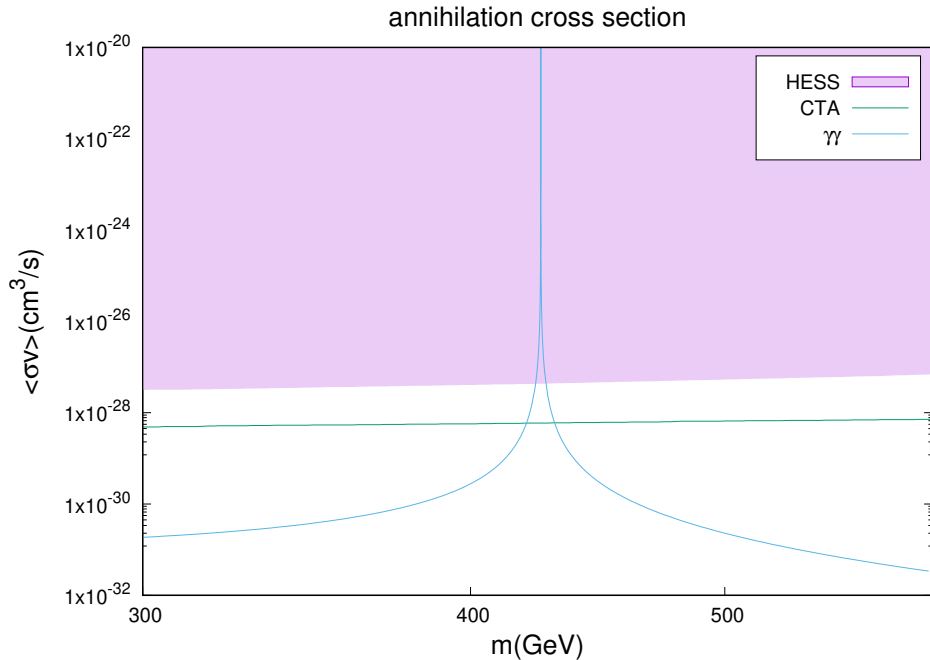


FIG. 9: A comparison of the cross section for  $\delta m = 3$  MeV in the coannihilation region with the HESS result [39] and projected CTA sensitivity [40]. The blue-solid line shows the calculation result, and the purple region shows the HESS result. The green-solid line shows the CTA sensitivity.

Next, we discuss the result of comparing DMs annihilation to  $\chi\chi \rightarrow \tau^+\tau^-$  channel with HESS and Fermi-LAT experimental data is shown in Fig. 10.

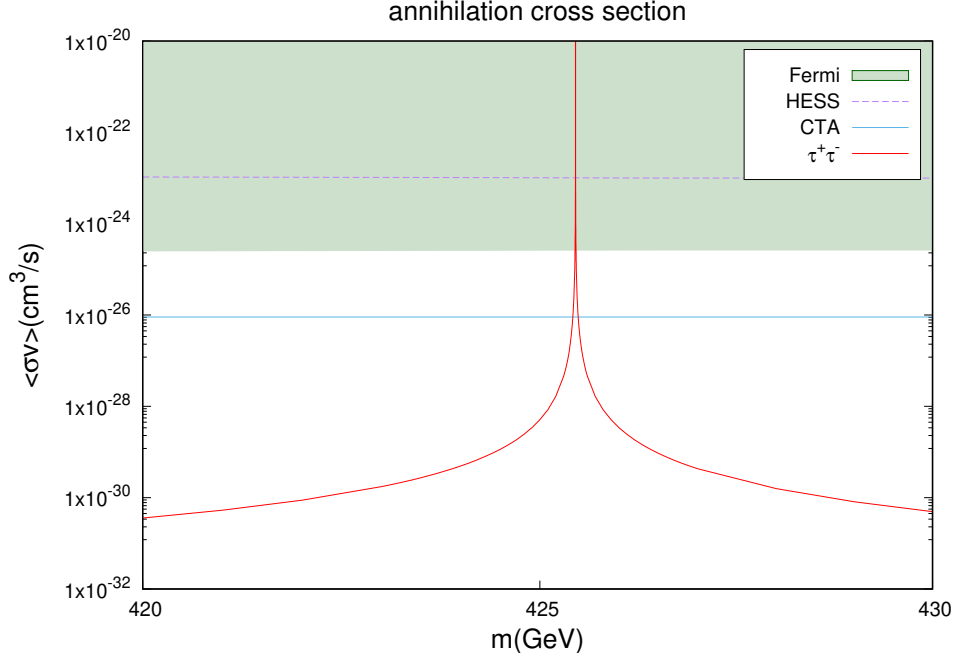


FIG. 10: A comparison of the cross section for  $\delta m = 3$  MeV for  $\tau^+\tau^-$  channel in the coannihilation region with the HESS result [20], Fermi-LAT result [30], and projected CTA sensitivity [40]. The red-solid line shows the calculation result, and the purple dotted-line shows the HESS result. The green area describes the upper limit by Fermi-LAT, and blue-solid line shows CTA sensitivity [40].

We also draw the projected CTA sensitivity line same as of  $\chi\chi \rightarrow \gamma\gamma$  case. Clearly, we cannot limit in most parameter region for  $\tau$  channel case, even for other channels. Thus we put the limitation of parameter region by using  $\chi\chi \rightarrow \gamma\gamma$  channel.

By applying the above-mentioned method to other  $\delta m$  cases as well, we can limit the parameter between  $\delta m$  and DM mass. The restricted parameter region is drawn in Fig. 11. In this figure, the blue-area describes the constrained region of our model.

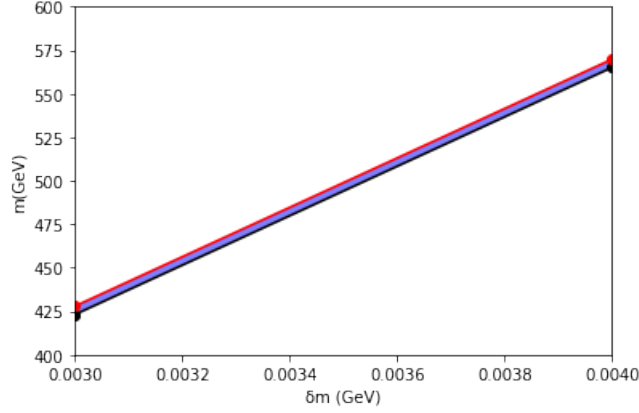


FIG. 11: The parameter region is limited by HESS experimental data. Parameters in colored areas are restricted.

We see that the narrow band in Fig. 11, which presents the limit from the current experimental restrictions on  $\delta m$ . In Fig. 12. we show that the future planned sensitivity of CTA that restricts about 100 times stronger than the present limit. It is found that the limit for  $\delta m$  can be set in a wide range in the future.

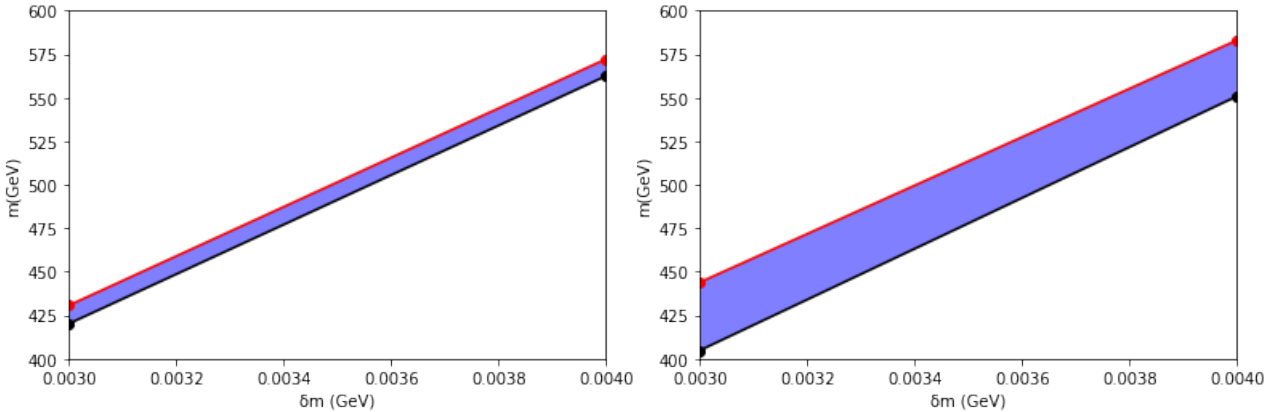


FIG. 12: The left graph corresponds to the limited parameter region constrained by projected CTA sensitivity. The right graph corresponds to the case where the limit is 100 times stronger. As experimental limits increase, more areas are restricted.

## V. CONCLUSION

We have investigated neutralino dark matter in the framework of MSSM. Hereby the mechanism of Sommerfeld enhancement is taken into account for the calculation of dark matter annihilation cross section and flux in the coannihilation region. In this region, if lepton flavor is violated, Lithium problem in cosmology is solved. The cross sections for several annihilation channels are shown in Fig. 5, Fig. 6 and Fig. 7: The dependence of  $\delta m$  on cross sections of  $\chi\tilde{\chi} \rightarrow \gamma\gamma$  channel is shown in Fig. 5. For  $\tilde{\chi}\tilde{\chi} \rightarrow ZZ$ ,  $\tilde{\chi}\tilde{\chi} \rightarrow W^+W^-$  and  $\tilde{\chi}\tilde{\chi} \rightarrow \tau^+\tau^-$  channel, cross sections are displayed in Fig. 6 and Fig. 7. It is revealed that these cross sections increase significantly due to Sommerfeld Enhancement in these figures. In Fig. 9, we compare our calculation result with the limits of current experimental data. Clearly, we can constrain the range of prohibited dark matter mass with the value of  $\delta m = 3$  MeV. We vary the value of  $\delta m$  from 3 MeV to 4 MeV then of course we get a similar limit comparing with the current experimental result as in Fig. 9. Further, we continue the same processes to vary the value of  $\delta m$  up to 10 MeV. Then finally all constraints on  $\delta m$  vs DM mass  $m$  are plotted in Fig. 11. On the left panel of Fig. 12, we show the limited parameter region acquired by comparing our result with future planned sensitivity of CTA [41, 42]. On the right panel of Fig. 12, we draw the disallowed parameter band which is obtained by comparison of the case of restricting about 100 times stronger according to the future planned experiments *e.g.* MAGIC [43].

In conclusion the cross section calculated by our model has already reached an observable range. Thus we can find signals from DM, and solve the problems such as dark matter and Li problems in the near future. In addition, even if no signal is detected, the parameters of the model can be limited and the validity of the supersymmetric particles can be verified soon.

### Acknowledgments

This work was supported by JSPS KAKENHI Grants No. JP18H01210 (J.S.), and MEXT KAKENHI Grant No. JP18H05543 (J.S.).

- 
- [1] Y. Fukuda *et al.*, Physical Review Letters **81**, 1562–1567 (1998).
- [2] D. M. Wittman, J. Tyson, D. Kirkman, I. Dell’Antonio, and G. Bernstein, Nature **405**, 143 (2000), arXiv:astro-ph/0003014.
- [3] WMAP, E. Komatsu *et al.*, Astrophys. J. Suppl. **192**, 18 (2011), arXiv:1001.4538.
- [4] Planck, N. Aghanim *et al.*, Astron. Astrophys. **641**, A6 (2020), arXiv:1807.06209.
- [5] J. R. Ellis, J. Hagelin, D. V. Nanopoulos, K. A. Olive, and M. Srednicki, Nucl. Phys. B **238**, 453 (1984).
- [6] G. Jungman, M. Kamionkowski, and K. Griest, Physics Reports **267**, 195–373 (1996).
- [7] S. G. Ryan, T. C. Beers, K. A. Olive, B. D. Fields, and J. E. Norris, Astrophys. J. Lett. **530**, L57 (2000), arXiv:astro-ph/9905211.
- [8] L. Sbordone *et al.*, Astron. Astrophys. **522**, A26 (2010), arXiv:1003.4510.
- [9] R. H. Cyburt, B. D. Fields, and K. A. Olive, JCAP **11**, 012 (2008), arXiv:0808.2818.
- [10] T. Jittoh *et al.*, Phys. Rev. D **76**, 125023 (2007), arXiv:0704.2914.
- [11] T. Jittoh *et al.*, Phys. Rev. D **78**, 055007 (2008), arXiv:0805.3389.
- [12] T. Jittoh *et al.*, Phys. Rev. D **82**, 115030 (2010), arXiv:1001.1217.
- [13] T. Jittoh *et al.*, Phys. Rev. D **84**, 035008 (2011), arXiv:1105.1431.
- [14] K. Kohri, S. Ohta, J. Sato, T. Shimomura, and M. Yamanaka, Phys. Rev. D **86**, 095024 (2012), arXiv:1208.5533.
- [15] Y. Konishi *et al.*, Phys. Rev. D **89**, 075006 (2014), arXiv:1309.2067.
- [16] J. Hisano, S. Matsumot, M. Nagai, O. Saito, and M. Senami, Physics Letters B **646**, 34–38 (2007).
- [17] J. R. Ellis, T. Falk, K. A. Olive, and M. Srednicki, Astropart. Phys. **13**, 181 (2000), arXiv:hep-ph/9905481, [Erratum: Astropart.Phys. 15, 413–414 (2001)].
- [18] N. Arkani-Hamed, D. P. Finkbeiner, T. R. Slatyer, and N. Weiner, Phys. Rev. D **79**, 015014 (2009), arXiv:0810.0713.
- [19] J. L. Feng, M. Kaplinghat, and H.-B. Yu, Phys. Rev. D **82**, 083525 (2010), arXiv:1005.4678.
- [20] H.E.S.S., A. Abramowski *et al.*, Phys. Rev. D **90**, 112012 (2014), arXiv:1410.2589.
- [21] Fermi-LAT, A. A. Abdo *et al.*, Phys. Rev. Lett. **102**, 181101 (2009), arXiv:0905.0025.
- [22] S. Biondini and S. Vogl, JHEP **02**, 016 (2019), arXiv:1811.02581.

- [23] C. El Aisati, C. Garcia-Cely, T. Hambye, and L. Vanderheyden, *JCAP* **10**, 021 (2017), arXiv:1706.06600.
- [24] HESS, H. Abdalla *et al.*, *JCAP* **11**, 037 (2018), arXiv:1810.00995.
- [25] E. Braaten, E. Johnson, and H. Zhang, *JHEP* **02**, 150 (2018), arXiv:1708.07155.
- [26] M. Lisanti, Lectures on Dark Matter Physics, in *Theoretical Advanced Study Institute in Elementary Particle Physics: New Frontiers in Fields and Strings*, pp. 399–446, 2017, arXiv:1603.03797.
- [27] J. Hisano, S. Matsumoto, M. M. Nojiri, and O. Saito, *Phys. Rev. D* **71**, 063528 (2005), arXiv:hep-ph/0412403.
- [28] S. Matsumoto, J. Sato, and Y. Sato, (2005), arXiv:hep-ph/0505160.
- [29] L. Bergstrom, P. Ullio, and J. H. Buckley, *Astropart. Phys.* **9**, 137 (1998), arXiv:astro-ph/9712318.
- [30] Fermi-LAT, M. Ackermann *et al.*, *Phys. Rev. Lett.* **115**, 231301 (2015), arXiv:1503.02641.
- [31] J. F. Navarro, C. S. Frenk, and S. D. M. White, *Astrophys. J.* **490**, 493 (1997), arXiv:astro-ph/9611107.
- [32] A. Burkert, *IAU Symp.* **171**, 175 (1996), arXiv:astro-ph/9504041.
- [33] A. W. Graham, D. Merritt, B. Moore, J. Diemand, and B. Terzic, *Astron. J.* **132**, 2685 (2006), arXiv:astro-ph/0509417.
- [34] J. F. Navarro *et al.*, *Mon. Not. Roy. Astron. Soc.* **402**, 21 (2010), arXiv:0810.1522.
- [35] M. Cirelli *et al.*, *JCAP* **03**, 051 (2011), arXiv:1012.4515, [Erratum: *JCAP* 10, E01 (2012)].
- [36] T. Sjöstrand *et al.*, *Comput. Phys. Commun.* **191**, 159 (2015), arXiv:1410.3012.
- [37] M. Kubo, J. Sato, T. Shimomura, Y. Takanishi, and M. Yamanaka, *Phys. Rev. D* **97**, 115013 (2018), arXiv:1803.07686.
- [38] ATLAS, M. Aaboud *et al.*, *Phys. Rev. D* **99**, 092007 (2019), arXiv:1902.01636.
- [39] HESS, H. Abdallah *et al.*, *Phys. Rev. Lett.* **120**, 201101 (2018), arXiv:1805.05741.
- [40] A. Hryczuk *et al.*, *JHEP* **10**, 043 (2019), arXiv:1905.00315.
- [41] CTA Consortium, R. A. Ong, *EPJ Web Conf.* **209**, 01038 (2019), arXiv:1904.12196.
- [42] CTA, A. Acharyya *et al.*, (2020), arXiv:2007.16129.
- [43] MAGIC, M. L. Ahnen *et al.*, *JCAP* **03**, 009 (2018), arXiv:1712.03095.

## Appendix A

For Lagrangian in (9), all terms are expressed as follows.

$$\begin{aligned}
\mathcal{L}_{KT} = & \frac{1}{2} \tilde{\chi} (i\partial - m) \tilde{\chi} + \tilde{C}_\alpha (i\partial - m_{C_\alpha}) \tilde{C}^\alpha + \bar{\nu}_D^i i\partial \nu_{Di} + \bar{e}^i \left( i\partial \delta_i^j - (m_e)_{i^j} \right) e_j \\
& - \tilde{\tau}^* (\partial^2 + m_{\tilde{\tau}}^2) \tilde{\tau} - \tilde{\nu}^{*i} (\partial^2 + m_{\tilde{\nu}}^2) \tilde{\nu}_i + \frac{1}{2} Z_\mu (\partial^2 + m_Z^2) Z^\mu \\
& + \frac{1}{2} A_\mu \partial^2 A^\mu + W_\mu^+ (\partial^2 + m_W^2) W^{\mu-} - \frac{1}{2} h^0 (\partial^2 + m_{h^0}^2) h^0,
\end{aligned} \tag{48}$$

where  $i, j = 1, 2, 3$  and

$$\mathcal{L}_{\text{int}} = \mathcal{L}_{\text{gauge}} + \mathcal{L}_{h^0-\tilde{\tau}-\tilde{\tau}} + \mathcal{L}_{h^0-h^0-\tilde{\tau}-\tilde{\tau}} + \mathcal{L}_{\text{gaugino}} + \mathcal{L}_{\text{chargino}}. \tag{49}$$

The details of each interaction term except  $\mathcal{L}_{\text{gauge}}$  are described below. In the following formula, the sums of  $i$  are taken from 1 to 3 and we consider the lightest neutralino and slepton only.

- Higgs-stau-stau 3-point interaction

$$\begin{aligned}
& \mathcal{L}_{h^0-\tilde{\tau}-\tilde{\tau}} \\
= & \frac{1}{\sqrt{2}} \tilde{\tau}^* \tilde{\tau} h^0 \left[ -\frac{1}{2} (c_\alpha v_u + s_\alpha v_d) \left( g^2 N_{\tilde{1}}^i N_{\tilde{1}}^{\dagger i 1} + g'^2 \left( -N_{\tilde{1}}^i N_{\tilde{1}}^{\dagger i 1} + 2N_{\tilde{1}}^{i+3} N_{\tilde{1}}^{\dagger i+3 1} \right) \right) \right. \\
& + 2s_\alpha v_d \left( N_{\tilde{1}}^i y_i^{\dagger k} y_k^j N_{\tilde{1}}^{\dagger j 1} + N_{\tilde{1}}^{i+3} y_i^k y_k^{\dagger j} N_{\tilde{1}}^{\dagger j+3 1} \right) \\
& \left. + c_\alpha \left( \mu^* N_{\tilde{1}}^{i+3} y_i^j N_{\tilde{1}}^{\dagger j 1} + h.c. \right) + s_\alpha \left( N_{\tilde{1}}^{i+3} a_i^j N_{\tilde{1}}^{\dagger j 1} + h.c. \right) \right]. \tag{50}
\end{aligned}$$

- Higgs-stau-stau 4-point interaction

$$\begin{aligned}
& \mathcal{L}_{h^0-h^0-\tilde{\tau}-\tilde{\tau}} \\
= & \tilde{\tau}^* \tilde{\tau} h^0 \left[ -\frac{1}{8} g^2 (c_\alpha^2 - s_\alpha^2) N_{\tilde{1}}^i N_{\tilde{1}}^{\dagger i 1} - \frac{1}{8} g'^2 (c_\alpha^2 - s_\alpha^2) \left( -N_{\tilde{1}}^i N_{\tilde{1}}^{\dagger i 1} + 2N_{\tilde{1}}^{i+3} N_{\tilde{1}}^{\dagger i+3 1} \right) \right. \\
& \left. - \frac{1}{2} s_\alpha^2 \left( N_{\tilde{1}}^i y_i^{\dagger k} y_k^j N_{\tilde{1}}^{\dagger j 1} + N_{\tilde{1}}^{i+3} y_i^k y_k^{\dagger j} N_{\tilde{1}}^{\dagger j+3 1} \right) \right]. \tag{51}
\end{aligned}$$

- Gaugino-interaction

$$\begin{aligned}
\mathcal{L}_{\text{gaugino}} = & \tilde{\tau}^* \tilde{\chi} \left[ P_L \left( \frac{\sqrt{2}}{2} g' N_{\tilde{1}}^i N_{\tilde{G}1}^1 + \frac{\sqrt{2}}{2} g N_{\tilde{1}}^i N_{\tilde{G}1}^2 + \frac{1}{2} N_{\tilde{1}}^{j+3} y_j^i N_{\tilde{G}1}^4 \right) \right. \\
& \left. + P_R \left( -\sqrt{2} g' N_{\tilde{1}}^{i+3} N_{\tilde{G}1}^1 + \frac{1}{2} N_{\tilde{1}}^i y_i^{\dagger j} N_{\tilde{G}1}^4 \right) \right] e_{Di} + h.c. \tag{52}
\end{aligned}$$



where,  $P_L, P_R$  is projection operator given as

$$P_L = \frac{1 - \gamma_5}{2}, \quad P_R = \frac{1 + \gamma_5}{2}. \quad (53)$$

Also, four-component spinors  $e_{Di}, \tilde{\psi}_{Da}^0$  are defined as

$$e_{Di} = \begin{pmatrix} e_{L\alpha i} \\ e_{R\dot{\alpha} i} \end{pmatrix}, \quad \tilde{\psi}_{Da}^0 = \begin{pmatrix} \tilde{\psi}_{\alpha a}^0 \\ \tilde{\psi}_{\dot{\alpha} a}^{0\dagger} \end{pmatrix}.$$

- Interaction between neutrino and chargino to release neutrino in the final state

$$\begin{aligned} \mathcal{L}_{\text{chargino}} &= -g\tilde{e}_L^* \tilde{W}^- \nu_i - g\nu^\dagger \tilde{W}^- \tilde{e}_{Li} - \frac{1}{2}\tilde{e}_R^* y_i^j \nu_j \tilde{H}_d^- - \frac{1}{2}\nu^\dagger y_i^j \tilde{e}_{Rj} \tilde{H}_d^{-\dagger} \\ &= \tilde{\tau}^* \tilde{C}_\alpha P_L \nu_{Di} \left[ -gN_{\tilde{1}}^i U_1^{\dagger\alpha} - \frac{1}{2}N_{\tilde{1}}^{j+3} y_j^i U_2^{\dagger\alpha} \right] + h.c., \end{aligned} \quad (54)$$

where four-component spinor  $\tilde{C}^\alpha$  is

$$\tilde{C}^\alpha = \begin{pmatrix} \tilde{C}_\alpha^+ \\ \tilde{C}^{-\dagger\alpha} \end{pmatrix}.$$

In Eq.(9), main terms are chosen.

## Appendix B

We note the result of integrating out the fields other than  $A_\mu$ . In the following formula, the sums of  $i$  is taken from 1 to 3.

- Effective action obtained by integrating out  $Z_\mu$

$$\begin{aligned}
\mathcal{S}_Z = & 2ie^2g_z^2 \left( s_w^2 - \frac{1}{2}N_{\tilde{l}1}^i N_{\tilde{l}i}^{\dagger 1} \right)^2 \\
& \times \text{tr} \int d^4x_1 d^4x_2 |\tilde{\tau}|^2(x_1) |\tilde{\tau}|^2(x_2) D_{\mu\nu}^Z(x_1 - x_2) D^{A\nu\rho}(x_2 - x_1) \\
& + ig_z^4 \left( s_w^2 - \frac{1}{2}N_{\tilde{l}1}^i N_{\tilde{l}i}^{\dagger 1} \right)^4 \\
& \times \text{tr} \int d^4x_1 d^4x_2 |\tilde{\tau}|^2(x_1) |\tilde{\tau}|^2(x_2) D_{\mu\nu}^Z(x_1 - x_2) D^{Z\nu\rho}(x_2 - x_1) \\
& + \frac{i}{2} \int d^4x d^4y J_Z^\mu(x) D_{\mu\nu}^Z(x - y) J_Z^\nu(y),
\end{aligned} \tag{55}$$

where

$$D_{\mu\nu}^Z(x - y) = -i \int \frac{d^4q}{(2\pi)^4} \frac{g_{\mu\nu}}{q^2 - m_Z^2 + i\epsilon} e^{-iq(x-y)}, \tag{56}$$

$$J_Z^\mu(x) = -ig_z \left( s_w^2 - \frac{1}{2}N_{\tilde{l}1}^i N_{\tilde{l}i}^{\dagger 1} \right) \tilde{\tau}^* \overleftrightarrow{\partial}^\mu \tilde{\tau}. \tag{57}$$

- Effective action obtained by integrating out  $W^+, W^-$

$$\begin{aligned}
\mathcal{S}_W = & \frac{i}{4}g^4 \left( N_{\tilde{l}1}^i N_{\tilde{l}i}^{\dagger 1} \right)^2 \text{tr} \int d^4x_1 d^4x_2 |\tilde{\tau}|^2(x_1) |\tilde{\tau}|^2(x_2) D_{\mu\nu}^W(x_1 - x_2) D^{W\nu\rho}(x_2 - x_1) \\
& + i \int d^4x d^4y J_W^\mu(x) D_{\mu\nu}^W(x - y) J_W^{\nu\dagger}(y),
\end{aligned} \tag{58}$$

where

$$D_{\mu\nu}^W(x - y) = -i \int \frac{d^4q}{(2\pi)^4} \frac{g_{\mu\nu}}{q^2 - m_W^2 + i\epsilon} e^{-iq(x-y)}, \tag{59}$$

$$J_W^\mu(x) = -i \frac{\sqrt{2}}{2} g N_{\tilde{l}1}^i \tilde{\tau}^* \overleftrightarrow{\partial}^\mu \tilde{\nu}_i, \tag{60}$$

$$J_W^{\mu\dagger}(x) = -i \frac{\sqrt{2}}{2} g N_{\tilde{l}i}^{\dagger 1} \tilde{\nu}^{*i} \overleftrightarrow{\partial}^\mu \tilde{\tau}. \tag{61}$$

- Effective action obtained by integrating out  $\tilde{\nu}^{*i}, \tilde{\nu}_i$

$$\begin{aligned} \mathcal{S}_{\tilde{\nu}} = & 2ig^4 N_{\tilde{l}i}^\dagger N_{\tilde{l}1} N_{\tilde{l}k}^\dagger N_{\tilde{l}1}^\dagger \text{tr} \int d^4x_1 d^4x_2 d^4x_3 d^4x_4 \\ & \times \partial^\sigma \tilde{\tau}^*(x_1) \partial^\mu \tilde{\tau}(x_2) \partial^\nu \tilde{\tau}^*(x_3) \partial^\rho \tilde{\tau}(x_4) \\ & \times D_{\tilde{\nu}j}^{\tilde{\nu}i}(x_1 - x_2) D_{\mu\nu}^W(x_3 - x_2) D_{\tilde{l}^k}^{\tilde{\nu}}(x_3 - x_4) D_{\rho\sigma}^W(x_1 - x_4), \end{aligned} \quad (62)$$

where

$$D_{\tilde{\nu}i}^{\tilde{\nu}j}(x - y) = -i \int \frac{d^4q}{(2\pi)^4} \frac{\delta_i^j}{q^2 - m_{\tilde{\nu}}^2 + i\epsilon} e^{-iq(x-y)}. \quad (63)$$

- Effective action obtained by integrating out  $e_D, \bar{e}_D$

$$\mathcal{S}_e = i \int d^4x d^4y \tilde{\tau}^*(x) \tilde{\tau}(y) \tilde{\chi}(x) [C_1^i P_L + C_2^i P_R] S^\tau(x - y)_i^j [C^\dagger_{1j} P_R + C^\dagger_{2j} P_L] \tilde{\chi}(y), \quad (64)$$

where

$$S^\tau(x - y)_i^j = i \int \frac{d^4q}{(2\pi)^4} \frac{\not{q} \delta_i^j + (m_e)_i^j}{q^2 - m_e^2 + i\epsilon} e^{-iq(x-y)}, \quad (65)$$

$$C_1^i = \left( \frac{\sqrt{2}}{2} g' N_{\tilde{l}1}^i N_{\tilde{G}1}^1 + \frac{\sqrt{2}}{2} g N_{\tilde{l}1}^i N_{\tilde{G}1}^2 + \frac{1}{2} N_{\tilde{l}1}^{j+3} y_j^i N_{\tilde{G}1}^4 \right), \quad (66)$$

$$C_2^i = \left( -\sqrt{2} g' N_{\tilde{l}1}^{i+3} N_{\tilde{G}1}^1 + \frac{1}{2} N_{\tilde{l}1}^i y_j^\dagger N_{\tilde{G}1}^4 \right). \quad (67)$$

- Effective action obtained by integrating out  $\nu_D, \bar{\nu}_D$

$$\mathcal{S}_{\tilde{\nu}} = i \int d^4x d^4y \tilde{\tau}^*(x) \tilde{\tau}(y) \tilde{C}_\alpha(x) C^{i\alpha} P_L S^\nu(x - y)_i^j C_{j\beta}^\dagger P_R \tilde{C}^\beta(y), \quad (68)$$

where

$$S^\nu(x - y)_i^j = i \int \frac{d^4q}{(2\pi)^4} \frac{\not{q} \delta_i^j}{q^2 + i\epsilon} e^{-iq(x-y)}, \quad (69)$$

$$C^{i\alpha} = -g N_{\tilde{l}1}^i U_1^{\dagger\alpha} - \frac{1}{2} N_{\tilde{l}1}^{j+3} y_j^i U_2^{\dagger\alpha}. \quad (70)$$

- Effective action obtained by integrating out  $\tilde{C}, \tilde{C}$

$$\begin{aligned} \mathcal{S}_{\tilde{C}} = & \frac{i}{2} \text{tr} \int d^4x_1 d^4x_2 d^4x_3 d^4x_4 \tilde{\tau}^*(x_1) \tilde{\tau}(x_2) \tilde{\tau}^*(x_3) \tilde{\tau}(x_4) \\ & \times S^{\tilde{C}}(x_1 - x_2)_\alpha^\beta C^{i\alpha} P_L S^\nu(x_2 - x_3)_i^j C_{j\beta}^\dagger P_R S^{\tilde{C}}(x_3 - x_4)_\gamma^\delta C^{k\gamma} P_L S^\nu(x_4 - x_1)_k^l C_{l\delta}^\dagger P_R, \end{aligned} \quad (71)$$

where

$$S^{\bar{C}}(x-y)_\alpha^\beta = i \int \frac{d^4 q}{(2\pi)^4} \frac{\not{q} + m_{C_\alpha}}{q^2 - m_{C_\alpha}^2 + i\epsilon} \delta_\alpha^\beta e^{-iq(x-y)}. \quad (72)$$

- Effective action obtained by integrating out  $h^0$

$$\begin{aligned} \mathcal{S}_{h^0} = & iC_{h^0}^{(4)2} \text{tr} \int d^4 x_1 d^4 x_2 |\tilde{\tau}|^2(x_1) |\tilde{\tau}|^2(x_2) D^{h^0}(x_1 - x_2) D^{h^0}(x_2 - x_1) \\ & - \frac{i}{2} \int d^4 x d^4 y J^{h^0}(x) D^{h^0}(x - y) J^{h^0}(y), \end{aligned} \quad (73)$$

where

$$\begin{aligned} D^{h^0}(x-y) &= -i \int \frac{d^4 q}{(2\pi)^4} \frac{1}{q^2 - m_{h^0}^2 + i\epsilon} e^{-iq(x-y)}, \\ J^{h^0}(x) &= |\tilde{\tau}(x)|^2 C_{h^0}, \end{aligned}$$

$$\begin{aligned} C_{h^0}^{(4)} = & -\frac{1}{8} g^2 (c_\alpha^2 - s_\alpha^2) N_{\tilde{l}1}^i N_{\tilde{l}i}^{\dagger 1} - \frac{1}{8} g'^2 (c_\alpha^2 - s_\alpha^2) \left( -N_{\tilde{l}1}^i N_{\tilde{l}i}^{\dagger 1} + 2N_{\tilde{l}1}^{i+3} N_{\tilde{l}i+3}^{\dagger 1} \right) \\ & - \frac{1}{2} s_\alpha^2 \left( N_{\tilde{l}1}^i y_i^\dagger{}^k y_k^j N_{\tilde{l}j}^{\dagger 1} + N_{\tilde{l}1}^{i+3} y_i^k y_k^\dagger{}^j N_{\tilde{l}j+3}^{\dagger 1} \right), \end{aligned} \quad (74)$$

$$\begin{aligned} C_{h^0} = & \frac{1}{\sqrt{2}} \left[ -\frac{1}{2} (c_\alpha v_u + s_\alpha v_d) \left( g^2 N_{\tilde{l}1}^i N_{\tilde{l}i}^{\dagger 1} + g'^2 \left( -N_{\tilde{l}1}^i N_{\tilde{l}i}^{\dagger 1} + 2N_{\tilde{l}1}^{i+3} N_{\tilde{l}i+3}^{\dagger 1} \right) \right) \right. \\ & + 2s_\alpha v_d \left( N_{\tilde{l}1}^i y_i^\dagger{}^k y_k^j N_{\tilde{l}j}^{\dagger 1} + N_{\tilde{l}1}^{i+3} y_i^k y_k^\dagger{}^j N_{\tilde{l}j+3}^{\dagger 1} \right) \\ & \left. + c_\alpha \left( \mu^* N_{\tilde{l}1}^{i+3} y_i^j N_{\tilde{l}j}^{\dagger 1} + h.c. \right) s_\alpha \left( N_{\tilde{l}1}^{i+3} a_i^j N_{\tilde{l}j}^{\dagger 1} + h.c. \right) \right]. \end{aligned} \quad (75)$$

Furthermore, we note

$$\begin{aligned} \mathcal{S}'_A = & ie^4 \text{tr} \int d^4 x_1 d^4 x_2 |\tilde{\tau}|^2(x_1) |\tilde{\tau}|^2(x_2) D_{\mu\nu}^A(x_1 - x_2) D^{A\nu\rho}(x_2 - x_1) \\ & + \frac{i}{2} \int d^4 x d^4 y J_A^\mu(x) D_{\mu\nu}^A(x - y) J_A^\nu(y), \end{aligned} \quad (76)$$

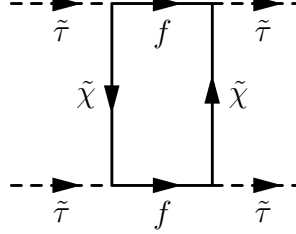
$$\mathcal{S}'_W = \frac{i}{4} g^4 \left( N_{\tilde{l}1}^i N_{\tilde{l}i}^{\dagger 1} \right)^2 \text{tr} \int d^4 x_1 d^4 x_2 |\tilde{\tau}|^2(x_1) |\tilde{\tau}|^2(x_2) D_{\mu\nu}^W(x_1 - x_2) D^{W\nu\rho}(x_2 - x_1), \quad (77)$$

where

$$J_A^\mu(x) = ie\tilde{\tau}^* \overleftrightarrow{\partial}^\mu \tilde{\tau}. \quad (78)$$

## Appendix C

For the calculation of the imaginary part, the result is as follows for the fields other than  $\mathcal{S}_\gamma$ . For example, a diagram in which fermions mediate is shown the below diagram.



With optical theorem, effective action of this case becomes

$$\begin{aligned}
\mathcal{S}_e &= \frac{i}{16\pi} \frac{(1 - m_e^2/m^2)^{3/2}}{(2m^2 - m_e^2)^2} [(|C_1|^2 + |C_2|^2)(m_e^2 + m(m_c + m_c^\dagger)) + m_c m_c^\dagger + m^2|C_1|^2|C_2|^2] \\
&\times \int d^4x \eta^*(x) \eta(x) \xi^*(x) \xi(x) \\
&\equiv i \Gamma_{e_i e_i} \int d^4x \eta^*(x) \eta(x) \xi^*(x) \xi(x).
\end{aligned} \tag{79}$$

For other fields,

$$\begin{aligned}
\mathcal{S}_Z &= i \left[ \frac{2g_z^4 \left( s_w^2 - \frac{1}{2} N_{\tilde{l}1}^i N_{\tilde{l}i}^{\dagger 1} \right)^4 m^6}{\pi m_z^4} \frac{\left( 1 - \frac{m^2}{m^2} \right)^{\frac{5}{2}}}{(m^2 + m_{\tilde{\tau}}^2 - m_z^2)^2} + \frac{g_z^4 \left( s_w^2 - \frac{1}{2} N_{\tilde{l}1}^i N_{\tilde{l}i}^{\dagger 1} \right)^4}{8\pi m^2} \sqrt{1 - \frac{m_z^2}{m^2}} \right] \\
&\times \int d^4x \eta^*(x) \eta(x) \xi^*(x) \xi(x) \\
&\equiv i \Gamma_{Z^0 Z^0} \int d^4x \eta^*(x) \eta(x) \xi^*(x) \xi(x),
\end{aligned} \tag{80}$$

where the sums of  $i$  is taken from 1 to 3.

$$\begin{aligned}
\mathcal{S}_{AZ} &= i \frac{e^2 g_z^2 \left( s_w^2 - \frac{1}{2} N_{\tilde{l}1}^i N_{\tilde{l}i}^{\dagger 1} \right)^2}{4\pi m^2} \left( 1 - \frac{m_z^2}{4m^2} \right) \int d^4x \eta^*(x) \eta(x) \xi^*(x) \xi(x) \\
&\equiv \Gamma_{\gamma Z^0} \int d^4x \eta^*(x) \eta(x) \xi^*(x) \xi(x).
\end{aligned} \tag{81}$$

$$\begin{aligned}
\mathcal{S}_W &= i \left[ \frac{g^4 \left( N_{l1}^i N_{\tilde{l}i}^{\dagger 1} \right)^4 m^6}{8\pi m_W^4} \left( 1 - \frac{m_W^2}{m^2} \right)^{\frac{5}{2}} \frac{1}{(m^2 + m_{\tilde{\nu}}^2 - m_W^2)^2} + \frac{g^4 \left( N_{l1}^i N_{\tilde{l}i}^{\dagger 1} \right)^4}{16\pi m^2} \sqrt{1 - \frac{m_W^2}{m^2}} \right] \\
&\quad \times \int d^4x \eta^*(x) \eta(x) \xi^*(x) \xi(x) \\
&\equiv i \Gamma_{W^+W^-} \int d^4x \eta^*(x) \eta(x) \xi^*(x) \xi(x). \tag{82}
\end{aligned}$$

$$\begin{aligned}
\mathcal{S}_\nu &= i \frac{\left( C^{i\alpha} C_{i\alpha}^\dagger \right)^2}{32\pi} \frac{m_{C_\alpha}^2}{(m^2 + m_{C_\alpha}^2)^2} \int d^4x \eta^*(x) \eta(x) \xi^*(x) \xi(x) \\
&\equiv i \Gamma_{\nu_i \nu_i} \int d^4x \eta^*(x) \eta(x) \xi^*(x) \xi(x). \tag{83}
\end{aligned}$$

$$\begin{aligned}
\mathcal{S}_{h^0} &= i \left[ \frac{C_{h^0}^4}{4\pi m^2} \sqrt{1 - \frac{m_{h^0}^2}{m^2}} \frac{1}{(m^2 + m_\tau^2 - m_{h^0}^2)^2} + \frac{C_{h^0}^{(4)4}}{32\pi m^2} \sqrt{1 - \frac{m_{h^0}^2}{m^2}} \right] \\
&\quad \times \int d^4x \eta^*(x) \eta(x) \xi^*(x) \xi(x) \\
&\equiv i \Gamma_{h^0 h^0} \int d^4x \eta^*(x) \eta(x) \xi^*(x) \xi(x). \tag{84}
\end{aligned}$$